Highly Efficient Thermal Decomposition of Volatile Organic Compounds by $Pt/CeO_2/ZSM\text{-}5$

Kojirou Fuku, Masahiko Goto, Takashi Kamegawa, Kohsuke Mori, and Hiromi Yamashita*

Division of Materials and Manufacturing Science, Graduate School of Engineering, Osaka University, 2-1 Yamadaoka, Suita, Osaka 565-0871

Received April 26, 2011
E-mail: yamashita@mat.eng.osaka-u.ac.jp

Small Pt nanoparticles were deposited on bifunctional CeO_2/ZSM-5 support combining noble metal stabilizing ability and adsorptive enrichment of organic molecules. The highly efficient thermal catalytic decomposition of methanol as a model compound of VOC can be achieved under mild conditions by $Pt/CeO_2/ZSM\text{-}5$.

Science and technology have contributed to the development of human society and a comfortable standard of living. However, various environmental problems such as global warming and air and/or water pollution have become international issues. Therefore, the production of valuable materials by energy conserving processes and efficient disposal of harmful chemical wastes are highly anticipated. Catalyst materials have been widely utilized to resolve these problems, and significant efforts have recently been devoted for achieving efficient organic synthesis and disposal of harmful chemical wastes by thermal catalytic and photocatalytic reaction.[1–16] Above all, noble metals such as Rh, Pt, and Pd play a very important role as beneficial catalyst metals for versatile reactions, such as hydrogenation, dehydrogenation, and oxidation decomposition.[11–16] However, these noble metals are very expensive with costs gradually increasing. In order to minimize the quantity of consumed noble metals, the development of catalyst materials exhibiting high catalytic activity with a small amount of noble metal is strongly desired.

In general, metal nanoparticles have been supported on various metal oxides such as SiO_2, Al_2O_3, and TiO_2 to reduce the quantity of consumed metal and promote reliable and durable catalytic activity.[17–19] Recently, preparation of composite catalyst materials such as noble metal particle-loaded zeolite has attracted much attention because zeolites have high thermal and chemical stability, high surface area of 300 to 600 $m^2 g^{-1}$, micropore structure of 4 to 12 Å, high catalytic ability and display high adsorption of organic molecules, especially volatile organic compound (VOC).[20–23]

We have previously reported a novel technique to prepare highly active Pt nanoparticles on ZSM-5 zeolite including cerium oxides,[24] in which efficient CO oxidation was achieved at low temperature by thermal catalytic effect of Pt/CeO_2 and the high surface area of ZSM-5. It is well known that the interaction between noble metal particles and metal oxides such as CeO_2, ZrO_2, Al_2O_3, and SiO_2 effectively maintains Pt particle size during catalytic reaction.[25] Particularly, since CeO_2 shows strong interaction with noble metal particles, i.e., stabilizing ability of these metals, and high oxygen storage capacity, CeO_2 is widely utilized in various applications such as cocatalyst in automobile three-way catalysts. It is herein demonstrated that combining the adsorptive ability of organic molecules originating from ZSM-5 zeolite enables high oxidative degradation efficiency at low temperature when methanol is used as a model VOC.

Results and Discussion

Table 1 shows the specific surface area and pore size of various catalyst materials obtained by N_2 adsorption–desorption measurement. The ZSM-5 zeolite possesses high surface area, but the specific surface area and pore size slightly decreased after the deposition of Pt particles. It is thought that Pt particles were formed on ZSM-5 zeolite, but high surface area remained even after Pt deposition. In the XRD pattern of $Pt/CeO_2/ZSM\text{-}5$, the peak due to CeO_2 (cubic) phases was observed slightly and the crystal size of CeO_2 calculated by Scherrer's equation was determined to be about 29 nm. However, the Pt nanoparticles were not observed by this XRD measurement. This indicates that small and highly dispersed Pt nanoparticles were supported on Pt/CeO_2/ZSM-5. TEM images of $Pt/CeO_2/ZSM\text{-}5$ and Pt/ZSM-5 are shown in Figure 1. The relatively small and highly dispersed Pt nanoparticles were supported on CeO_2/ZSM-5, and the diameter of the Pt nanoparticles was ca. 5–10 nm (Figure 1A). On the other hand, Pt nanoparticles with a wide size distribution were formed on the ZSM-5 and the Pt nanoparticles supported on ZSM-5 were bigger than that supported on CeO_2/ZSM-5 (Figure 1B). It has been reported that the interaction between Pt nanoparticles and CeO_2 is stronger than that between Pt nanoparticles and ZSM-5 supports, which inhibit the aggregation of Pt nanoparticles.[25] In addition, Table 2 shows the dispersion and particle size of Pt metals calculated by pulsed CO adsorption. The Pt particle size decreased in the order of $Pt/ZSM\text{-}5 > Pt/CeO_2/ZSM\text{-}5 > Pt/CeO_2$. These results indicate that addition of CeO_2 is a useful way to support small Pt particles on various supports. The obtained Pt particles were also characterized by Pt L_{III}-edge XAFS spectra (Figure 2). The XANES spectra of all samples are similar to that of Pt foil, suggesting the presence of Pt in a metallic state. In the Fourier transforms of Pt

Table 1. The Summarized Results on Surface Structure Obtained Using N_2 Adsorption/Desorption Measurement

Sample	S_{BET} /$m^2 g^{-1}$	Pore volume /$cm^3 g^{-1}$
CeO_2	157	—
ZSM-5	408	0.18
Pt/CeO_2	118	—
Pt/ZSM-5	383	0.18
$Pt/CeO_2/ZSM\text{-}5$	370	0.17

Published on the web August 4, 2011; doi:10.1246/bcsj.20110119

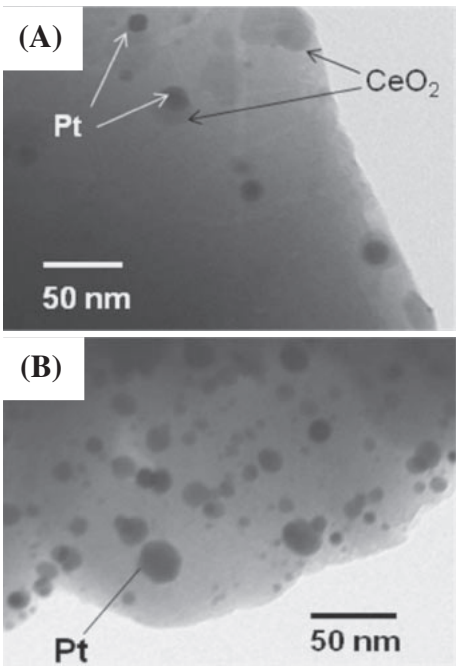

Figure 1. TEM images of (A) $Pt/CeO_2/ZSM-5$ and (B) Pt/ZSM-5.

Table 2. The Dispersion and Particle Size of Pt Metals of Various Pt-Supported Catalysts Determined by the Pulsed CO Adsorption Measurement

Sample	Dispersion /%	Particle size /nm
Pt/CeO_2	67	1.7
Pt/ZSM-5	8	14.2
$Pt/CeO_2/ZSM-5$	18	6.1

L_{III}-edge EXAFS spectra, all samples exhibited a peak at approximately 2.7 Å due to the contiguous Pt–Pt bond in the metallic form nanoparticles. The peak intensity also decreased in the order of $Pt/ZSM-5 > Pt/CeO_2/ZSM-5 > Pt/CeO_2$, which is due to the smaller particle size of the Pt. The order of peak intensity was in close agreement with the order of the Pt particle size calculated by the pulsed CO adsorption. These results indicate that aggregation of Pt nanoparticles on CeO_2 was inhibited by interaction between Pt nanoparticles and CeO_2.

The comparison of catalytic activity using various catalysts was carried out by methanol oxidation. Figure 3 shows the effect of various Pt nanoparticle-loaded catalysts on complete methanol decomposition at 323 K. The reaction hardly occurred when bare ZSM-5 and CeO_2 were used as catalysts. In addition, CeO_2-loaded ZSM-5 ($CeO_2/ZSM-5$) also hardly exhibited decomposition activity of methanol, indicating that these bare catalysts are inactive for methanol decomposition in the absence of Pt nanoparticles. On the other hand, CO_2 was observed at low temperature in the presence of Pt nanoparticle-loaded catalysts such as Pt/ZSM-5, Pt/CeO_2, and $Pt/CeO_2/ZSM-5$. This suggests that supported Pt worked as the active site for the methanol oxidation. The catalytic activity toward methanol decomposition increased in the order of $Pt/CeO_2 < Pt/ZSM-5 < Pt/CeO_2/ZSM-5$. It should be noted that $Pt/CeO_2/ZSM-5$

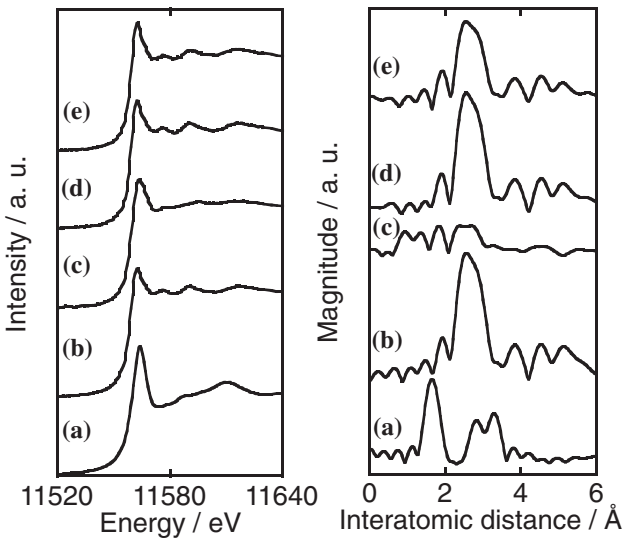

Figure 2. Pt L_{III}-edge XANES spectra (left) and FT-EXAFS spectra (right) of (a) PtO_2, (b) Pt foil, (c) Pt/CeO_2, (d) Pt/ZSM-5, and (e) $Pt/CeO_2/ZSM-5$.

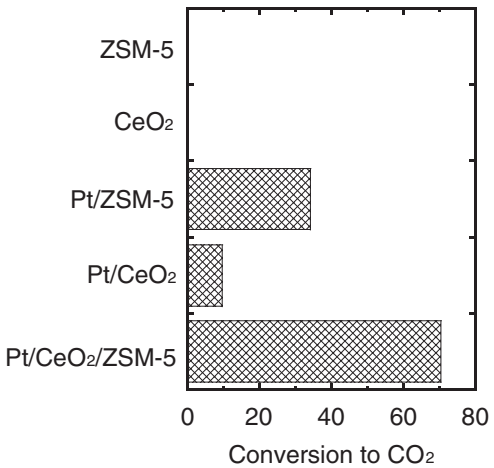

Figure 3. The comparison of catalytic activity for methanol complete decomposition using various catalysts (Reaction temperature: 323 K).

including a small part of CeO_2 showed the high methanol decomposition activity compared with other samples. It is believed that specifically high methanol decomposition was achieved at low temperature by the synergenic effect of relatively small Pt nanoparticles highly dispersed on CeO_2 and adsorptive enrichment of methanol by ZSM-5. On the other hand, although very small Pt nanoparticles were supported on CeO_2, the Pt/CeO_2 sample exhibited low decomposition activity, indicating that adsorptive enrichment by CeO_2 is poorer than that of ZSM-5. Since $Pt/CeO_2/ZSM-5$ exhibited efficient oxidative decomposition activity even under mild reaction conditions, it is suggested that utilization of CeO_2-loaded ZSM-5 as catalyst support would be a promising strategy for the loading of small Pt nanoparticles as well as energy-saving disposal of harmful organic materials such as VOC.

In conclusions, small Pt nanoparticles could be deposited on $CeO_2/ZSM-5$ support by the metal stabilizing ability of CeO_2 and highly efficient methanol decomposition was achieved

under mild reaction conditions by the $Pt/CeO_2/ZSM\text{-}5$ catalyst supporting a small quantity of CeO_2.

Experimental

All reagents were commercial materials of reagent grade and used without further purification.

Preparation of CeO_2-Loaded ZSM-5. The loading of CeO_2 was performed by impregnation (Imp) method. ZSM-5 (molar ratio of $SiO_2/Al_2O_3 = 1900$) was suspended in an aqueous solution of $Ce(NO_3)_3 \cdot 6H_2O$ in a flask and stirred at room temperature for 2 h. After evaporation to dryness at 343 K, the resultant powder was dried at 373 K for 16 h under air and then calcined at 773 K for 5 h in air, resulting in the formation of $CeO_2/ZSM\text{-}5$ (CeO_2: 5 wt %).

Preparation of Pt-Loaded CeO_2/ZSM-5. Pt nanoparticles were also deposited by Imp method. After $CeO_2/ZSM\text{-}5$ was suspended in an aqueous solution of $H_2[PtCl_6]$ in a flask and stirred at room temperature for 2 h, the flask was evaporated to dryness at 343 K. The resultant powder was dried under vacuum for 16 h and then calcined at 723 K for 5 h in air, resulting in the formation of $Pt/CeO_2/ZSM\text{-}5$ (Pt: 1 wt %). In comparison, the Pt deposition on CeO_2 (JRC-CEO-1) and ZSM-5 was also performed using Imp method (Pt/CeO_2 and Pt/ZSM-5, Pt: 1 wt %).

Characterization. Powder X-ray diffraction (XRD) patterns were recorded on a Rigaku Ultima IV X-ray diffractometer using Cu Kα radiation ($\lambda = 1.5406$ Å) over the range of 10–50°. Specific surface area and pore distribution measurements using N_2 adsorption–desorption were performed BELSORP-max (BEL Japan, Inc.) at 77 K. The measurement samples were pretreated under H_2 flow at 673 K for 20 min and were degassed under vacuum at 323 K prior to data collection. CO pulse adsorption was performed to measure Pt dispersion and particle size by BEL-METAL-1 (BEL Japan, Inc.). The measurement samples were pretreated under He flow at 673 K for 15 min, O_2 flow at 673 K for 15 min, and subsequently H_2 flow at 673 K for 15 min. The CO adsorption was measured at 323 K and CO flow rate was 20 $cm^3\,min^{-1}$. The Pt L_{III}-edge X-ray absorbance fine structure (XAFS) spectra of these catalysts were measured in fluorescence mode with an attached Si(111) monochromator at the BL01B1 station at Spring-8, Harima, Japan. TEM image was obtained with a Hitachi H-800 electron microscope equipped with an energy-dispersive X-ray (EDX) detector, operated at 200 kV.

Catalytic Reaction. The methanol oxidation was carried out at 323 K using a distributive reactor vessel. The catalyst (50 mg) was placed in a quartz-tube reactor and pretreated under O_2 flow at 673 K for 20 min, and subsequently H_2 flow at 673 K for 20 min. A mixed gas of air and methanol (35 $\mu mol\,min^{-1}$) was supplied at a flow rate of 20 $cm^3\,min^{-1}$ in the quartz-tube reactor. The amount of CO_2 produced by complete oxidative decomposition of methanol was measured using a Shimadzu GC-8A gas chromatograph equipped with Porapak Q and Porapak S columns.

This study was financially supported by Grants-in-Aid for Scientific Research and from Ministry of Education, Culture, Sports, Science and Technology of Japan (No. 20360363) and Global COE Program (Project: Center of Excellence for Advanced Structural and Function Materials Design) from Ministry of Education, Culture, Sports, Science and Technology of Japan. The X-ray absorption experiments were performed at the BL01B1 station of SPring-8 (prop. No. 2010A1540). The authors appreciate Dr. Eiji Taguchi and Prof. Hirotaro Mori at the Research Center for Ultra-High Voltage Electron Microscopy, Osaka University for assistance with TEM measurements.

References

1 V. A. Kondratenko, U. Bentrup, M. Richter, T. W. Hansen, E. V. Kondratenko, *Appl. Catal., B* **2008**, *84*, 497.
2 Y. Ukisu, *J. Hazard. Mater.* **2008**, *152*, 287.
3 Z. Zhang, Y. Liu, L. Ling, Y. Li, Y. Dong, M. Gong, X. Zhao, Y. Zhang, J. Wang, *J. Am. Chem. Soc.* **2011**, *133*, 4330.
4 J. M. Thomas, R. Raja, D. W. Lewis, *Angew. Chem., Int. Ed.* **2005**, *44*, 6456.
5 K. Fuku, K. Hashimoto, H. Kominami, *Chem. Commun.* **2010**, *46*, 5118.
6 K. Fuku, K. Hashimoto, H. Kominami, *Catal. Sci. Technol.* **2011**, *1*, 586.
7 K. Mori, M. Kawashima, M. Che, H. Yamashita, *Angew. Chem., Int. Ed.* **2010**, *49*, 8598.
8 I. Ryu, A. Tani, T. Fukuyama, D. Ravelli, M. Fagnoni, A. Albini, *Angew. Chem., Int. Ed.* **2011**, *50*, 1869.
9 T. Kamegawa, J. Morishima, M. Matsuoka, J. M. Thomas, M. Anpo, *J. Phys. Chem. C* **2007**, *111*, 1076.
10 K. Mori, Y. Miura, S. Shironita, H. Yamashita, *Langmuir* **2009**, *25*, 11180.
11 H. Yamashita, K. Mori, *Chem. Lett.* **2007**, *36*, 348.
12 J. Sun, H. Liu, *Green Chem.* **2011**, *13*, 135.
13 B. Bridier, J. Pérez-Ramírez, *J. Am. Chem. Soc.* **2010**, *132*, 4321.
14 G. Novell-Leruth, A. Valcárcel, J. Pérez-Ramírez, J. M. Ricart, *J. Phys. Chem. C* **2007**, *111*, 860.
15 J. A. Hernandez, S. Gómez, B. Pawelec, T. A. Zepeda, *Appl. Catal., B* **2009**, *89*, 128.
16 K. Ikeue, K. Murakami, S. Hinokuma, K. Uemura, D. Zhang, M. Machida, *Bull. Chem. Soc. Jpn.* **2010**, *83*, 291.
17 E. Bus, J. A. van Bokhoven, *Phys. Chem. Chem. Phys.* **2007**, *9*, 2894.
18 D. K. Liguras, D. I. Kondarides, X. E. Verykious, *Appl. Catal., B* **2003**, *43*, 345.
19 G. Martra, L. Prati, C. Manfredotti, S. Biella, M. Rossi, S. Coluccia, *J. Phys. Chem. B* **2003**, *107*, 5453.
20 A. C. Akah, G. Nkeng, A. A. Garforth, *Appl. Catal., B* **2007**, *74*, 34.
21 J.-Y. Wang, F.-Y. Zhao, R.-J. Liu, Y.-Q. Hu, *J. Mol. Catal. A: Chem.* **2008**, *279*, 153.
22 R. Krishna, J. M. van Baten, *Langmuir* **2010**, *26*, 10854.
23 Y. Ichihashi, Y. Kamizaki, N. Terai, K. Taniya, S. Tsuruya, S. Nishiyama, *Catal. Lett.* **2010**, *134*, 324.
24 S. Shironita, M. Goto, T. Kamegawa, K. Mori, H. Yamashita, *Catal. Today* **2010**, *153*, 189.
25 Y. Nagai, T. Hirabayashi, K. Dohmae, N. Takagi, T. Minami, H. Shinjoh, S. Matsumoto, *J. Catal.* **2006**, *242*, 103.